DESIGN OF HYBRID HEAT AND POWER CO-GENERATION SYSTEM

by

Yingai JIN[a,b], Mingjie LV[a,b], Yuying YAN[c], and Mingyu QUAN[a,b]*

[a] State Key Laboratory of Automotive Simulation and Control, Jilin University, Changchun, China
[b] College of Automotive Engineering, Jilin University, Changchun, China
[c] Faculty of Engineering, University of Nottingham, University Park, Nottingham, UK

Original scientific paper
https://doi.org/10.2298/TSCI2205119J

The energy revolution considering renewable power is indispensable and inevitable in the development of modern power industry, yet has been restricted by many practical problems. The instability of renewable energy makes the whole power generation system unable to maintain stable output, which causes fluctuations in the power grid system, and ultimately affects the user side. Also, there are few researches on hybrid heat and power co-generation system and when applied to the regional power supply, current systems converse electric energy to thermal energy to meet the heating demand of users, which reduces the energy quality. Hybrid two or more kinds of renewable energy is a way to eliminate instability of renewable energy power generation system. In this paper, a hybrid heat and power co-generation system is designed to reach both heat and power demands of users, a solar-geothermal power generation system was simulated on ASPEN PLUS platform. The output power, entropy and energy efficiency are analyzed to optimize the system. Based on the solar-geothermal power generation system, exergy analysis shows that the parallel heating and power generating system is much more efficient than the original system.

Key words: *solar energy, geothermal energy, hybrid heat and power, exergy analysis, parallel heating and power*

Introduction

The high use of fossil fuels has led to environmental issues such as GHG emission and climate changes in the recent years, therefore, renewable energy is proposed as an alternative to replace fossil fuels [1]. The use of sustainable energy has become ever important and increasing necessary in the 21st century [2]. Hybridization of solar thermal and geothermal energy has been considered in [3]. The renewable and sustainable energy resources have received enormous interest in the last decade due to their potential of sustainability. Individual renewable energy technologies have their own unique characteristics. Hybridization of different technologies may result in a more efficient and cost-effective system than simply co-locating individual technologies [4]. Rosato *et al.* [5] used software TRNSYS to simulate a centralized solar hybrid heating and cooling system. The results show that energy consumption can be saved up to 40.2%. Gimellia *et al.* [6] have done a lot of work in the field of combined heat and power (CHP). A method for grid-connected co-generation devices assisted by

* Corresponding author, e-mail: mingyuquan96@gmail.com

battery energy storage is proposed and the energy and economic performance are evaluated in detail. The performance of a waste heat recovery device was evaluated, a system for matching the temperature level required by the user with the temperature level provided by the power plant is introduced [7]. The reliability of the gas turbine thermodynamic model is verified and compared it with experimental data [8]. Kilkis *et al.* [9] have developed an exergy-based holistic model for district energy system and determined the optimum mix of renewables. Calise *et al.* [10] established a dynamic simulation model of the cogeneration system on TRNSYS, and carried out a detailed economic analysis. Torres *et al.* [11] redesigned the reflector geometry in hybrid concentrating collectors to improve the energy efficiency of the solar collectors. The results show its performance is significantly improved compared with the current standard concentrating solar collector system. Heberle *et al.* [12] presented a thermo-economic analysis for a low-temperature organic Rankine cycle (ORC) in a combined CHP generation case. Lee *et al.* [13] compared the heating performance of hybrid ground-source heat pump in series and parallel configurations and conducted an experimental analysis on the heating performance of hybrid heat pumps with a series-parallel hybrid structure. He *et al.* [14] proposed a hybrid power supply system with a high proportion of renewable energy and analyzed the rationality and functionality of the hybrid power system in detail. Yucer *et al.* [15] analyzed a steam heating system based on the Second law of thermodynamics to explore its potential for improvement in reducing exergy consumption, fuel consumption and cost. Through the use of exergy parameters to improve the heating system, provides relatively simple solutions and investment advice to reduce heat loss, fuel consumption and costs. Zhang *et al.* [16] combined the advantages of solar and geothermal heat pump hybrid system and analyzed the energy-saving potential of the system.

It can be known from the aforementioned paper review that the existing system only aims at the demand of power generation, while the current user demand is the coexistence of heating demand and power supply demand. If the system only supplies power and converts electric energy into heat, there will be energy grade decline in the intermediate process, resulting in irreversible loss, and energy utilization is neither scientific nor efficient.

In this paper, a hybrid solar-geothermal power generation system was modeled on ASPEN PLUS platform, which is shown in fig. 1. On the basis of this model, the system is optimized to make the hybrid solar-geothermal power generation system changed from a single electrical power generation system to a parallel heating electrical power generation system. According to the efficiency analysis and exergy analysis, the efficiency of the system and the work done by the system can be obtained to analyzed the advantages of the system.

Methods

Modeling of the holistic system: the solar-geothermal power generation system basically contains photovoltaic generating set and geothermal generating set. The system includes conversion devises and storage with the input and output of multiple energy carriers such as electricity, gas, heating, and cooling.

Structure of solar-geothermal power generation system is shown in fig. 1.

The thermal conductive oil flows through the ET150 solar collector plate, and is used as a heat source to exchange heat with the geothermal fluid in the heat exchanger SH, and then flows through the pump SP to pressurize into the solar collector plate, forming a circulation as an auxiliary heat source for geothermal energy. The geothermal fluid first exchanges heat with the thermal oil through the heat exchanger SH, the temperature increases, and then flows through the flash valve. After flashing, it enters the gas-liquid separator DIV.

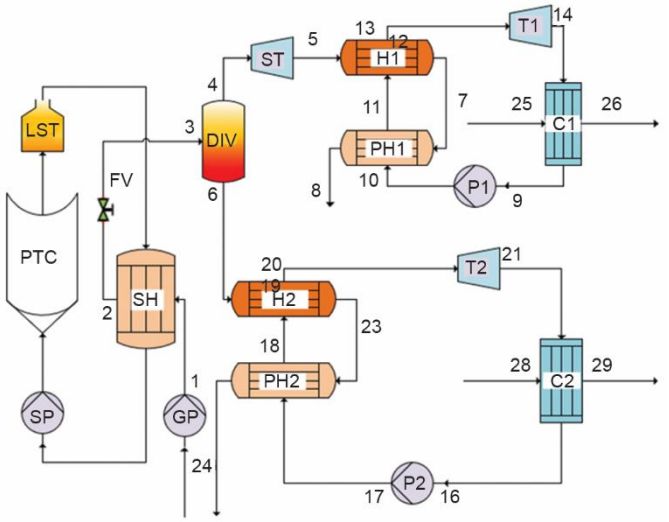

Figure 1. Structure of solar-geothermal power generation system; *PTC – solar collector, SP – solar pump, GP – geothermal energy pump, SH – solar heat exchanger, DIV – flash tank, ST – steam turbine, FV – flash valve, LST – liquid storage tank, H1 – upper heat exchanger, PH1 – upper preheater, T1 – upper turbine, C1 – upper condenser, P1 – upper pressure pump, H2 – lower heat exchanger, PH2 – lower preheater, T2 – turbine, C2 – lower condenser, P2 – lower pressure pump*

The fluid in the gas-liquid separator is divided into two paths: high temperature and high pressure steam – 4 flows in the first path. The high-temperature and high-pressure steam flows from the outlet of the gas-liquid separator into the steam turbine ST to perform work, and then flows through the heater H1 as the heat source of the upper ORC, and then flows through the preheater PH1, then back to the ground. The high temperature water – 6 flows in the second path. As the heat source of the lower ORC, the high temperature and high-pressure water directly enters the superheater H2, then enters the preheater PH2, and then flows to underground.

The upper ORC uses isopentane (i-C_5H_{12}) as the working fluid. The working fluid is first preheated by the preheater PH1, then enters the superheater H1 to be superheated to high temperature and high pressure steam, and then enters the turbine T1 for work, and then enters the condensers C1 for condensation. The condensed liquid enters the pump P1 for pressurization and then enters the preheater to complete a cycle. The lower ORC uses butane (C_4H_{10}) as the working fluid. The cycle process of lower part is the same as the upper part. The working fluid is first preheated by the preheater PH2, then enters the superheater H2 to be superheated to high temperature and high pressure steam, then enters the turbine T2 for work, then enters the condensers C2 for condensation, and the condensed liquid working fluid enters the pump P2 for pressurization and then enters the preheater to complete a cycle.

The *T-s* diagram of the solar preheating system and the upper ORC is shown in fig. 2. In the preheating process, the working fluid is heated to saturated liquid state by the thermal conductive oil (1-2). The saturated liquid undergoes the flash evaporation process (2-3) to reach the liquid-vapor saturation state, then it undergoes the liquid-vapor separator process and separates into saturated steam (4) and saturated liquid (6) and saturated steam expands in the turbine to produce work (4-5). The upper ORC is 9-10-11-12-13-14-9, which is made up of the following six processes: organic working fluid pressurization process (9-10), preheating process (10-11), evaporation process (11-12), overheating process (12-13), work process (13-14), and condensation process (14-9).

Figure 3 shows the *T-s* diagram of the lower ORC of the geothermal energy, which is made up of the following six processes: organic working fluid pressurization process (16-17),

preheating process (17-18), evaporation process (18-19), overheating process (19-20), work process (20-21), and condensation process (21-16).

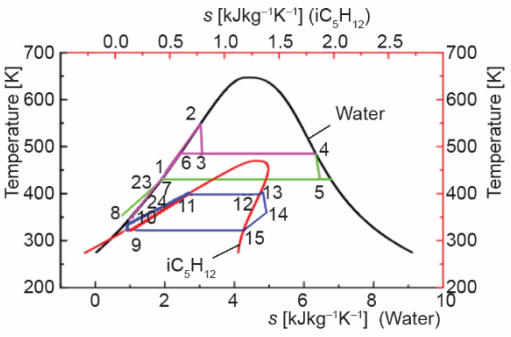

Figure 2. The *T-s* diagram of the solar preheating system and the upper ORC

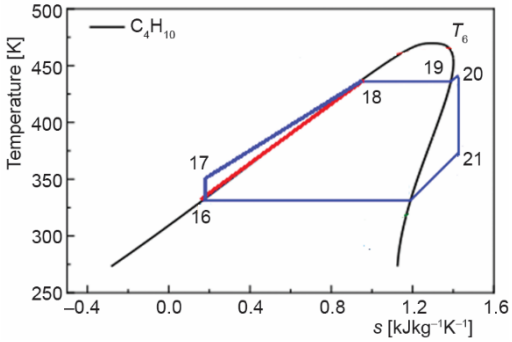

Figure 3. The *T-s* diagram of the lower ORC of the geothermal energy

In the solar preheated geothermal fluid system, the trough solar collector performs heat conversion by absorbing solar energy. The solar energy is concentrated on the heat exchange tube through the reflection of the heat collector plate, and the heat transfer is carried out with the heat transfer oil in the heat exchange tube. The absorbed heat of the trough solar system can be mainly defined [17]:

$$\dot{Q}_{\text{abs}} = A_{\text{a}} I_b (\cos\theta)\eta \tag{1}$$

$$\eta = KMN\left(A + B\frac{\Delta T}{2}\right) + (C + Dw)\frac{\Delta T}{2I_b} \tag{2}$$

where A_{a} [m^2] is the area of the solar field, I_b [kJh^{-1}m^{-2}] – the direct solar radiation intensity, θ [°] – the angle of incidence, η [–] – the absorption efficiency, K [–] – the incident angle modification factor, M [–] – the final loss factor, and N [–] – the factor considering parallel shadows, A, B, C, D_W are empirical coefficients, and ΔT [K] – the difference between the thermal oil temperature and the ambient temperature.

The heat transfer model of the solar heat collector can be simplified:

$$Q_{\text{solar}} = DNI\ A_{\text{solar}} \tag{3}$$

$$Q_{\text{collector}} = DNI\ A_{\text{solar}} \cdot \eta_{\text{opt}} - Q_{\text{loss}} \tag{4}$$

where Q_{solar} [kJ] is the total solar radiation energy obtained by the radiation in the solar collector, DNI [kJm^{-2}] – the direct irradiation intensity of solar radiation, A_{solar} [m^2] – the heat exchange area of the solar collector, $Q_{\text{collector}}$ [kJ] – the actual heat that can be obtained by the heat transfer oil in the heat exchange pipe of the solar collector, Q_{loss} [kJ] – the heat loss generated by solar energy in the process of photothermal conversion, and η_{opi} [–] – the absorption coefficient.

$$\eta_{\text{solar}} = \frac{Q_{\text{collector}}}{Q_{\text{solar}}} \tag{5}$$

$$\eta_{\text{system}} = \frac{Q_{\text{solar}}}{Q_{\text{system}}} \tag{6}$$

where η_{solar} is the heat collection efficiency of the solar collector and η_{system} – the ratio of the solar energy input energy in the system to the total input energy of the system.

The adiabatic compression process in the solar preheating system leads to entropy increase. The isentropic efficiency and power consumption are:

$$\eta_{is,SP} = \frac{h_{26s} - h_{25}}{h_{26} - h_{25}} \tag{7}$$

$$W_{SP} = m_{25}\frac{h_{26s} - h_{25}}{\eta_{is,SP}}\eta_{me,pump} = m_{25}\left(h_{26} - h_{25}\right)\eta_{me,pump} \tag{8}$$

$$\eta_{is,GP} = \frac{h_{0s} - h_1}{h_0 - h_1} \tag{9}$$

$$W_{GP} = m_0\frac{h_{0s} - h_1}{\eta_{is,GP}}\eta_{me,pump} = m_0\left(h_0 - h_1\right)\eta_{me,pump} \tag{10}$$

where $\eta_{is,SP}$ and $\eta_{is,GP}$ are the isentropic efficiency of SP and GP, respectively, $\eta_{me,pump}$ – the mechanical efficiency of the pump, and W_{SP}, W_{GP} – the power consumption of solar circulating pumps and geothermal water pumps, respectively.

The system exergy balance equation can be expressed:

$$E_i = m_i[(h_i - h_0) - T_0(S_i - S_0)] \tag{11}$$

$$E_{solar} + E_{geothermal} + E_{GP} + E_{SP} = E_2\Delta E_{collector,d}\Delta E_{GP,d} + \Delta E_{exchanger,d} \tag{12}$$

$$E_{solar} = DNI\ A\,\eta_{opt}IAM(\theta)\left(1 - \frac{T_0}{T_s}\right) \tag{13}$$

where S_i [kJK^{-1}kg^{-1}] and h_i [kJkg^{-1}] are the entropy and enthalpy at state i, respectively, S_0 and h_0 – the entropy and enthalpy of working fluid at the environment state, E_i – the exergy at the state point i, m_i – the mass flow at the state point i, E_{solar} [kJ] – the exergy obtained by the solar collector, $E_{geothermal}$ [kJ] – the geothermal energy input exergy, E_{GP} [kJ] – the input exergy of the geothermal fluid pump, E_{SP} [kJ] – the input exergy of the pump solar circulation pump, E_2 [kJ] – the exergy of of the fluid in state 2 in fig. 1, $\Delta E_{collector,d}$ [kJ] – the exergy destruction of the solar collector, $\Delta E_{GP,d}$ [kJ] – the exergy destruction of the geothermal fluid pump, $\Delta E_{exchanger,d}$ [kJ] – the heat exchanger exergy destruction, η_{opt} – the optical loss efficiency of the solar collector, $IAM(\theta)$ – the incident angle correction coefficient, T_0 and T_s [K] – the ambient temperature and solar surface temperature respectively.

In the upper ORC, the high temperature and high pressure steam flowing out of the upper part of the gas-liquid separator passes through the turbine to work. The isentropic efficiency of the turbine, the turbine for the amount of work and the exergy balance for flash expansion work can be expressed:

$$\eta_{i,ST} = \frac{h_{4s} - h_5}{h_4 - h_5} \tag{14}$$

$$W_{ST} = m_4\left(h_{4s} - h_5\right)\eta_{m,ST}\eta_{i,ST} = m_4\left(h_4 - h_5\right)\eta_{m,ST} \tag{15}$$

$$E_2 = W_{ST} + E_5 + E_6 + \Delta E_{f,dectruction} + \Delta E_{ST,dectruction} \tag{16}$$

where W_{ST} [kJ] is the work done by the turbine, $\eta_{m,ST}$ and $\eta_{i,ST}$ – the isentropic and mechanical efficiencies of the turbine, respectively, and h_{is} – the isentropy at the state point *i*.

The upper ORC uses the exhaust heat of the turbine as a heat source to provide heat for the organic working fluid. Therefore, the work done in the ORC, the pump power consumption in the ORC and the exergy balance model of the ORC can be expressed:

$$W_{P2} = m_{P2}(h_{10} - h_9)\eta_{m,P2} \tag{17}$$

$$\eta_{i,T2} = \frac{h_{13s} - h_{14}}{h_{13} - h_{14}} \tag{18}$$

$$W_{T2} = m_{T2}(h_{13} - h_{14})\eta_{m,T2} \tag{19}$$

$$W_{P2} = W_{T2} + E_8 - E_5 + \Delta E_{T2,dectruction} + \Delta E_{P2,dectruction} + \Delta E_{evap2,dectruction} +$$

$$+\Delta E_{cond2,dectruction} + \Delta E_{PH2,dectruction} \tag{20}$$

where W_{P2} and W_{T2} are the power of pump P2 and turbine T2 in the upper ORC system, respectively, $\eta_{i,T2}$ is the efficiency of the turbine T2 in the upper ORC.

In the lower ORC, the high temperature saturated water flowing out of the lower part of the gas-liquid separator is used as the heat source to work. The flow rate of the organic working fluid can be calculated by eq. (21). The two parameters are superheat and pinch point temperature difference, which can be calculated by eqs. (22) and (23), respectively. The work and efficiency of the system can be calculated by eqs. (24)-(26):

$$c_6 m_6 (T_{23} - T_6) = c_{19} m_{19} (T_{20} - T_{19}) \tag{21}$$

$$\Delta T_g = T_{20} - T_{19} \tag{22}$$

$$\Delta T_z = T_{23} - T_{19} \tag{23}$$

$$W_{P1} = m_{P1}(h_{17} - h_{16})\eta_{m,P1} \tag{24}$$

$$W_{T1} = m_{T1}(h_{20} - h_{21})\eta_{m,T1} \tag{25}$$

$$W_{P1} = W_{T1} + E_{23} - E_6 + \Delta E_{T1,dectruction} + \Delta E_{P1,dectruction} + \Delta E_{evap1,dectruction} +$$

$$+\Delta E_{cond1,dectruction} + \Delta E_{PH1,dectruction} \tag{26}$$

where W_{P1} and W_{T1} are the power of the pump P1 and the turbine T1 in the upper ORC system, respectively, $\eta_{i,T1}$ is the efficiency of the turbine T1 in the upper ORC.

Exergy calculation model of the heating and power generation system is:

$$W_{net} = W_{T1} + W_{T2} + W_{ST} - W_{P1} - W_{P2} - W_{SP} - W_{GP} \tag{27}$$

$$\eta_{th} = \frac{W_{net}}{Q_s + Q_g} \tag{28}$$

$$Q_g = m_0 h_0 - m_8 h_8 - m_{23} h_{23} \tag{29}$$

$$\eta_{ex} = \frac{W_{net}}{E_s + E_g} \tag{30}$$

$$E_s = m_0 e_0 - m_8 e_8 - m_{23} e_{23} \tag{31}$$

where W_{net} [kJ] is the net work of the heating and power generation system, η_{th} [–] – the thermal efficiency of the system, η_{ex} [–] – the exergy efficiency of the system, Q_s and Q_g – the heat input to the solar and geothermal energy systems, respectively, and E_s and E_g – the exergy values of solar and geothermal energy input systems, respectively.

The initial parameters of the solar-geothermal power generation system is shown in tab. 1.

Table 1. The initial parameters of the solar-geothermal power generation system

Warm-up cycle	Parameters	Flash work part	Parameters
Geothermal fluid temperature [°C]	200	Flash valve pressure [MPa]	2
Solar thermal conductive oil temperature [°C]	395	Gas-liquid separator tank pressure [MPa]	2
Preheat pump pressure [MPa]	4	Steam turbine back pressure [MPa]	0.5
Geothermal fluid preheat pump pressure [MPa]	6		
Upper circulation		Lower circulation	
Turbine back pressure [MPa]	0.15	Turbine back pressure [MPa]	0.2
Pump pressure [MPa]	1	Pump pressure [MPa]	1.5

In order to better meet the needs of users and improve energy efficiency, Configuration 1 is proposed, as shown in fig. 4. The working fluid (water) from the condenser outlet of

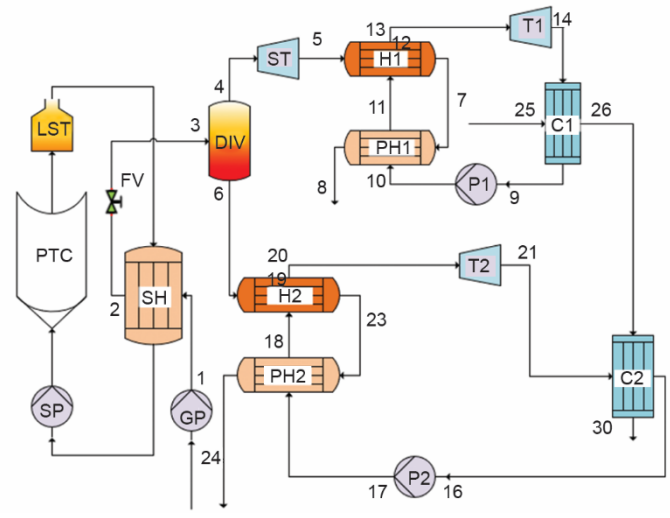

Figure 4. Parallel heating and power generating system, plant Configuration 1

the upper cycle is reheated in the lower cycle, thus increasing the temperature of the working fluid (water). Configuration 1 transformation does not involve reforming turbine, so there is no change in the amount of work done by the system. Due to the waste heat utilization of the system, the efficiency of the system is naturally improved.

For the greater heating demand in winter, a high temperature and high pressure fluid is drawn from the upper turbine middle section to heat the hydraulic working medium that has been reheated in Configuration 1, thus increasing the temperature of the hydraulic working medium again. An additional heat exchanger is placed in the lower ORC to heat water from the outlet of the upper heat exchanger. The working medium water flows through the four heat exchangers in turn, increasing the temperature of the water and finally reaching the water supply temperature, as shown in fig. 5, where C3 is upper heat exchanger, C4 is lower heat exchanger.

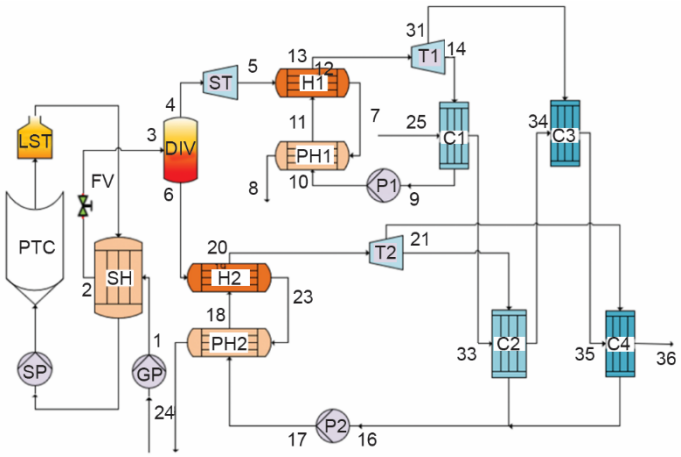

Figure 5. Parallel heating and power generating system, plant Configuration 2

Results

Through the simulation of solar-geothermal power generation system, the thermodynamic parameters of each unit of the system and the thermodynamic characteristics of the overall system are obtained. The net output power of the system was 12.76 MWh, thermal efficiency was 14.5% and exergy efficiency was 22.1%. Through the established thermodynamic model and according to the initial parameters and operating parameters of the system for mathematical calculation, the net output power of the system was 12.45 MWh, thermal efficiency was 14.2% and exergy efficiency was 21.8%. The maximum exergy loss of system exergy loss of solar collector is 16,377 kW, accounting for 47%. The second is the heat loss of preheater, 4105 kW, accounting for 12%. Exergy loss is mainly caused by condensation and heat transfer at the top and in the low and medium ORC, accounting for 7% to 9%.

Table 2 shows that the outlet working fluid temperature of the lower cycle turbine is about 110 °C, the outlet working fluid temperature of the upper cycle turbine is around 90 °C, the inlet water working fluid temperature of the upper condenser is around 5 °C, and the inlet water working fluid temperature of the lower condenser is 62.7 °C, water temperature at the outlet of the ORC condenser in the lower part of the system is 95.2 °C. Therefore, the Configuration 1 of the hybrid heat and power co-generation system can meet the requirements of heating users in winter. Table 3 shows that when the system is optimized, the final outlet tem-

perature of the wage water in the system after four heat exchangers is 110.1 °C. As cold stream exchanges heat multiple times, the heat exchange temperature difference is reduced, thereby the heat exchange loss of the heat exchanger is reduced. The water temperature increases greatly. It can meet the heating requirements for high temperature heating in winter.

Table 2. Fluid temperature of Configuration 1 system [°C]

Heat source		Condenser inlet		Condenser outlet	
Upper	90	Upper	5	Upper	63.4
Lower	110	Lower	62.7	Lower	95.2

Table 3. Fluid temperature of Configuration 2 system [°C]

Heat source		Condenser inlet		Condenser outlet		Heat exchanger heat source		Outlet water	
Upper	90	Upper	5	Upper	56.3	Upper	111	Upper	96.7
Lower	110	Lower	56.3	Lower	81.4	Lower	134	Lower	110.1

As shown in tab. 4, after the system is optimized according to plant Configuration 1, as the high temperature and high pressure fluid in the turbine works normally, the exergy value of the turbine in the system does not change. Because the system uses waste heat to continuously heat water through the heat exchanger, the utilization of waste heat is more fully, so the utilization of waste heat in the system leads to the increase of thermal exergy value of 2987.268 kW. As shown in tab. 5, after optimization of the system according to plant Configuration 2, exergy value of the steam turbine in the system decreased by 3101.27 kW because 15% high temperature and high pressure hot fluid is extracted from the upper and lower steam turbines in the system as the heat source to heat water without complete work. As the system uses waste heat for multistage heating of water, the utilization of waste heat makes the utilization of surplus heat in the system more fully, resulting in an increase of exergy value of 5485.75 kW.

Table 4. Plant Configuration 1 compared with the original system

	Work of original system [kW]	Work of work of plant configuration 1 [kW]	
Upper	–6123.48	–6123.48	
Lower	–4891.62	–4891.62	
Total work	–11015.11	–11015.11	
Waste heat utilization exergy [kW]		Exergy enhancement [kW]	Work difference [kW]
5674.384	2687.11	2987.26	0

Table 6 shows that work and exergy efficiency of Configuration 1 and Configuration 2. Exergy efficiency of parallel heating and power generating system, plant Configuration 1 is 28.4%. Exergy efficiency increases by 4%-5% compared to the solar-geothermal power generation system. Exergy efficiency of parallel heating and power generating system, plant Configuration 2 is 27.3%. Exergy efficiency increases by 3%-4% compared to the solar-geothermal power generation system.

Table 5. Plant Configuration 2 compared with the original system

	Work of original system [kW]	Work of work of plant configuration 2 [kW]	
Upper	–6123.48	–1648.91	–2080.12
Lower	–4891.62	–1850.24	–2334.54
Total work	–11015.11	–7913.83	
Waste heat utilization exergy [kW]		Exergy enhancement [kW]	Work difference [kW]
8172.874	2687.11	5485.75	3101.27

Table 6. Work and exergy efficiency of Configuration 1 and Configuration 2

Item / System	Work [kW]	Input exergy [kW]	Exergy efficiency [%]
Configuration 1	11015.12	57547.8	28.35602404
Configuration 2	7913.84	57547.8	27.30857906

Conclusions

Exergy loss is calculated for solar-geothermal power generation system and the changes of exergy loss in each part are obtained. Based on the calculation, it can be concluded that the greatest exergy loss in the system occurred in the solar preheating system, accounting for 47%. The second is solar preheater, exergy loss accounted for 12%.

After the transformation of system through the two Configurations, it is shown that the two configurations could not only provide heating, but also significantly increase the exergy utilization of the system. After optimization in Configuration 1, exergy efficiency of the system increases by 4-5%, resulting in water temperature of 95.2 ℃. After the system is optimized in Configuration 2, exergy usage of the system increases by 3-4% and higher water temperature is obtained, which is 110.1 ℃.

After the comparison of plant Configurations 1 and 2, it can be seen that Configuration 1 has a more significant improvement in exergy efficiency. However, the outlet water temperature obtained in Configuration 1 is low, which can only meet the requirements of ordinary heating but cannot meet the requirements of high temperature heating. Configuration 2 can meet the requirements of high temperature heating and water temperature, but the exergy efficiency is less improved than Configuration 1. Therefore, both Configurations 1 and 2 are ideal renovation schemes of heating parallel system. If the output temperature of Configuration 1 meets requirements, Configuration 1 is used as the preferred configuration. If the output temperature does not meet the requirements, Configuration 2 is preferred.

Acknowledgment

This work was supported by the Royal Academy of Engineering (UK) under the Newton Fund UK-China Industry Academia Partnership Program scheme (UK-CIAPP\201).

This work was supported by Jilin Province Science and Technology Development Plan Project (No. 20180414021GH).

References

[1] Parikhani, T., *et al.*, A Novel Geothermal Combined Cooling and Power Cycle Based on the Absorption Power Cycle: Energy, Exergy and Exergoeconomic Analysis, *Energy*, *153* (2018), 15, pp. 265-277

[2] Steven, C., Arun, M., Opportunities and Challenges for a Sustainable Energy Future, *Nature*, *488* (2012), 15, pp. 294-303
[3] Tempesti, D., Fiaschi, D., Thermo-Economic Assessment of a Micro CHP System Fueled by Geothermal and Solar Energy, *Energy, 58* (2013), 1, pp. 45-51
[4] McTigue, J. D., *et al.*, Assessing Geothermal/Solar Hybridization-Integrating a Solar Thermal Topping Cycle into a Geothermal Bottoming Cycle with Energy Storage. *Applied Thermal Engineering, 171* (2020), 5, pp. 115-121
[5] Rosato, A., *et al.*, Dynamic Simulation of a Solar Heating and Cooling System Including a Seasonal Storage Serving a Small Italian Residential District, *Thermal Science, 24* (2020), 6A, pp. 3555-3568
[6] Gimellia, A., *et al.*, Optimal Configuration of Modular Cogeneration Plants Integrated by a Battery Energy Storage System Providing Peak Shaving Service, *Applied Energy, 242* (2019), 15, pp. 974-993
[7] Gimellia, A., *et al.*, Performance Assessment of a 15 kW Micro-CHCP Plant through the 0D/1D Thermo-Fluid Dynamic Characterization of a Double Water Circuit Waste Heat Recovery System, *Energy, 181* (2019), 15, pp. 803-814
[8] Gimellia, A., *et al.*, A Vector Optimization Methodology Applied to Thermodynamic Model Calibration of a Micro Gas Turbine CHP Plant, *Energy Procedia, 148* (2018), Aug., pp. 2-9
[9] Kilkis, B., An Exergy-Rational District Energy Model For 100% Renewable Cities with Distance Limitations, *Thermal Science, 24* (2020), 6A, pp. 3685-3705
[10] Calise, F., *et al.*, Optimal Operating Strategies of Combined Cooling, Heating and Power Systems: A Case Study for an Engine Manufacturing Facility, *Energy Conversion and Management, 149* (2017), 1, pp. 1066-1084
[11] Torres, J. P. N., *et al.* Effect of the Collector Geometry in the Concentrating, *Thermal Science, 22* (2018), 5, pp. 2243-2256
[12] Heberle, F., Bruggemann, D., Thermoeconomic Analysis of Hybrid Power Plant Concepis for Geothermal Combined Heat and Power Generation, *Energies, 7* (2014), 7, pp. 4482-4497
[13] Lee, M., *et al.*, Comparative Heating Performance Evaluation of Hybrid Ground-Source Heat Pumps Using Serial and Parallel Configurations with the Application of Ground Heat Exchanger, *Energy Conversion and Management, 229* (2021), 1, pp. 1-11
[14] He, W. Z., *et al.*, Research on AC & DC Hybrid Power Supply System with High-Proportion Renewable Energy of Data Center, *The Journal of Engineering, 16* (2019), Mar., pp. 3230-3233
[15] Yucer, C. T., *et al.*, Improving the Performance of a Heating System through Energy Management by Using Exergy Parameters, *Thermal Science, 24* (2020), 6A, pp. 3771-3780
[16] Zhang, H., Zhang, H., Application of the Hybrid System of Solar Energy and Geothermal Heat Pump in Buildings, *Advanced Materials Research, 377* (2012), 374, pp 137-140
[17] Forristall, R. E., Heat Transfer Analysis and Modeling of a Parabolic Trough Solar Engineering Equation Solver, Tech. report, National Renewable Energy Laboratory, Golden, Cal., USA, 2003

Paper submitted: December 6, 2021
Paper revised: March 31, 2021
Paper accepted: April 23, 2022